International Journal of Design & Nature and Ecodynamics
Vol. 20, No. 11, November, 2025, pp. 2545-2555
Journal homepage: http://iieta.org/journals/ijdne

Chitosan-Cryogels Loaded with Lactic Acid Bacteria Supernatants Effectively Inhibit Uropathogenic *Escherichia coli* Biofilms and Virulence

Mohammed T. Abdul Hussein*, Basam Basim Mohammed, Tamara Abbas Hamed

Department of Microbiology, College of Science, Mustansiriyah University, Baghdad 10001, Iraq

Corresponding Author Email: tamara.a@uomustansiriyah.edu.iq

Copyright: ©2025 The authors. This article is published by IIETA and is licensed under the CC BY 4.0 license (http://creativecommons.org/licenses/by/4.0/).

https://doi.org/10.18280/ijdne.201106

Received: 15 September 2025
Revised: 6 November 2025
Accepted: 21 November 2025
Available online: 30 November 2025

Keywords:
UPEC, qPCR, outer membrane proteins, cryogels, cell-free supernatants, antibiofilm

ABSTRACT

Uropathogenic *Escherichia coli* (UPEC) is a primary causative agent of urinary tract infections (UTIs), often complicating treatment and recovery. This study involved the isolation and identification of UPEC strains from various clinical specimens collected at hospitals in Baghdad, including Al-Emam Ali Hospital and Al-Kindi Hospital. The investigation focused on evaluating the potential of chitosan-based cryogels, impregnated with cell-free supernatants (CFSs) derived from lactic acid bacteria (LAB), against clinical UPEC isolates. *Lactobacillus sporogenes* CFSs were prepared and incorporated into chitosan-based cryogels. Antibacterial activity was assessed using disc diffusion and broth dilution assays, along with evaluations of biofilm inhibition, ATP depletion, and lipid peroxidation. Additionally, the expression of virulence-associated genes was analyzed using real-time polymerase chain reaction (RT-PCR). Scanning electron microscopy (SEM) revealed that the synthesized cryogels featured a highly porous matrix. Significant antibacterial and antibiofilm effects were observed when compared to the positive control group ($p < 0.05$). Broth dilution assays demonstrated potent bactericidal activity, with the cryogels exhibiting a minimum inhibitory concentration (MIC) as low as 37.2 µg/mL ($p < 0.05$). Biofilm biomass was reduced by 83%, lipid peroxidation increased by 74%, and ATP levels declined by 61%. Furthermore, the expression of key virulence-related genes—*ompA*, *ompF*, *ompC*, and *tolC*—was downregulated by 13%, 12%, 32%, and 15%, respectively. These findings underscore the effectiveness of CFS-loaded cryogels as a promising therapeutic strategy against UPEC infections. The developed cryogels demonstrate strong potential as antimicrobial coatings for urinary catheters and wound dressings, offering an innovative approach for managing bacterial resistance and biofilm-associated complications.

1. INTRODUCTION

Urinary tract infections (UTIs) are some of the predominant bacterial diseases that occur globally and impact millions of people per year. They are a serious challenge to both clinical practice and the economy, particularly in developing countries, where such infections are ranked as the second most frequent nosocomial infections after those of the respiratory tract [1]. About 80% of the infections in the urinary tract are attributed to uropathogenic *Escherichia coli* (UPEC), which has been known to possess different kinds of virulence factors that include adhesion, invasion, and biofilm formation, thus resulting in persistence and resistance to antibiotics. The deposition of UPEC between the cells of the epithelium of the bladder leads to recurrent infections, reduced antibiotic effectiveness, and the need for new antimicrobial agents [2, 3]. Hence, interest is growing in creating novel biomaterial-mediated delivery systems that can efficiently reduce bacterial virulence and resistance development.

Chitosan-based cryogels refer to macroporous sponge-like materials that are prepared by freezing and freeze-drying chitosan solutions or at least chitosan-based polymers or nanoparticle solutions [4]. They are biocompatible, biodegradable, and inherently antibacterial, making them applicable in wound dressings, haemostatic agents, and controlled drug delivery systems [5]. They have a high porosity, three-dimensional structure that allows them to be highly absorbent of water and mechanically stable, containing cationic amino functionalities of chitosan interacting with anionic bacterial cell membranes to destabilize the membrane of cells and cause bacterial death [6-8]. Also, chitosan can chelate the essential metal ions and disrupt bacterial DNA replication, which offers several antibacterial modes of action.

The cell-free supernatant (CFS) derived from lactic acid

bacteria (LAB) is a potent antimicrobial agent, as it comprises an array of substances that include organic acids, bacteriocins, hydrogen peroxide, and enzymes whose mixture is capable of inhibiting most of the pathogens of the wide range of groups of microbes, like *E. coli*, *Salmonella* spp. and *Staphylococcus aureus* [9-11]. These bioactive agents lead to the rupture of bacterial membranes, the prevention of biofilm formation, and antioxidant and anti-inflammatory effects that together revive an eco-friendly and naturally antimicrobial alternative. LAB-CFS is also reported to disrupt the extracellular polymeric substance production and bacterial motility, which compromises the formation of the biofilm and the severity of infections [12]. Although the antimicrobial and antibiofilm potentials of both chitosan cryogels and LAB-CFS are significant alone. Their application in combination with each other has not been explored fully yet. It is expected that the incorporation of LAB-CFS into a chitosan cryogel matrix will be advantageous in the form of improved bioactivity of LAB-derived metabolites, with the structural stability and controlled-release ability of chitosan giving the bioactivity it possesses. This synergistic effect may be able to guarantee a sustained, localized antimicrobial effect, enhanced antibiofilm efficacy, and reduced development of bacterial resistance in comparison with each agent separately.

There is still no available study that has investigated this synergistic interaction, especially in comparison with clinically relevant UPEC strains. This study, thus, aimed at synthesizing chitosan-based cryogels that are conjugated with isolated LAB-CFS fractions and investigating their antibacterial, antibiofilm, and antivirulence properties against the UPEC isolates. The cryogels developed were scanned using scanning electron microscopy (SEM), and their biological activity was assessed using the broth dilution assay, biofilm inhibition assays, ATP production assay, and expression profiling of virulence genes using quantitative PCR. So, the current approach aims to fill a major gap by establishing how the antimicrobial and antivirulence activities of LAB-CFS can be synergistically boosted on chitosan cryogels to create a basis for their potential application as topical antimicrobial coatings for infection control.

2. MATERIALS AND METHODS

2.1 Materials

Samples collection: Isolates used were from MTCC 729. The study included isolation and identification of samples from different clinical sources in some Baghdad hospitals: Al-Emam Ali hospital, Alkendi hospital, and for the diagnosis of uropathogenic *E. coli* isolates (Figure 1).

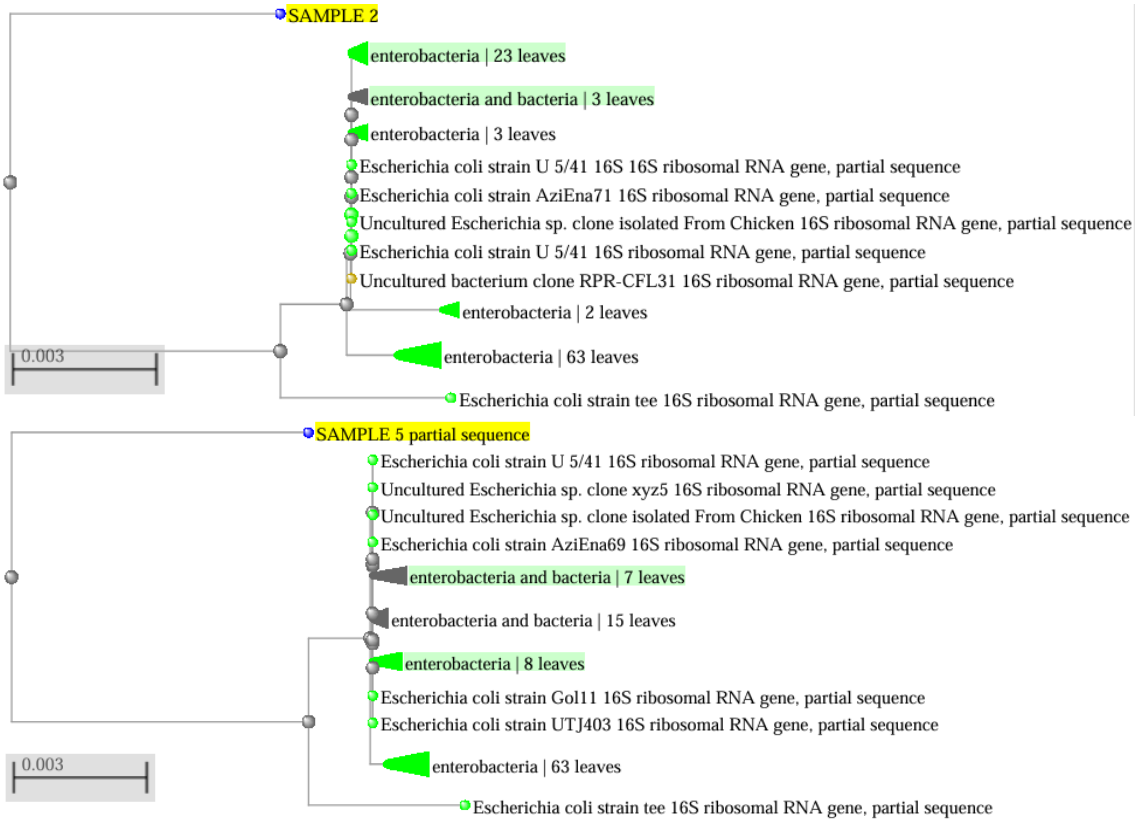

Figure 1. Phylogenetic tree and similarity of the isolated strains in the study

2.2 Methods

2.2.1 Preparation of cell-free supernatants of LAB

Cell-free supernatants were made following the protocol described by research [13], but with slight modifications. The experiment started with the addition of powder (later confirmed to be *Lactobacillus sporogenes*, a probiotic lactic acid bacterium based on the specification from the Sporlac sachet; Sanzyme Pvt Ltd, India), about 0.1 g, into 10 mL of MRS broth. The materials were then incubated at 37°C in an incubator. Following the period of incubation, about 100 µl of the starter culture was harvested and inoculated into 100 mL of MRS broth. The broth that was inoculated was then incubated for 2 days at 37°C. The suspension of the culture was filtered and centrifuged for 10 minutes at a rate of 8,000 rpm at 4°C. The obtained supernatant was again filtered using

0.2 m-sized cellulose filter paper, and finally, the CFS was utilized in the following synthesis process.

2.2.2 Fabrication of cryogels with CFS

Cryogels were prepared following the protocol described by research [14], but with slight modifications. Chitosan cryogels were prepared by adding about 0.2 g of chitosan (mid-range molecular weight, degree of deacetylation ~85%, Sigma-Aldrich) into 10 mL of acetic acid solution (6%). To prepare chitosan-based gelatine composite cryogels, gelatine was added at a 75:25 (w/w) ratio of chitosan to gelatine into the acetic acid–based chitosan preparations. The solution was then added to 2.5 mL of 6% (v/v) glutaraldehyde solution (final concentration) and mixed thoroughly in a magnetic stirrer. To the suspension, about 5 mL of CFS (undiluted) was added and mixed thoroughly with constant stirring for about 30 min.

The solution obtained was added to a 2.5 mL plastic syringe and incubated for 3 hr at -16℃. Following 3 hr incubation, the samples were maintained for a period of 24–48 hr in the freezer at −16℃. The resulting cryogels were taken out of the syringes and dissolved in distilled water to wash off the unreacted ingredients. Washing was carried out 3 times, and then freeze-dried. The dried powder obtained was then pulverized into fine powder form. The prepared samples were refrigerated at +4℃. The cryogels loaded with positive control (colistin, 10 mg/mL, free drug concentration equivalent to that incorporated into the cryogel) were similarly fabricated.

2.2.3 FTIR analysis

The obtained cryogels in powder form were characterized by Fourier transform infrared spectroscopy (FTIR) spectral analysis using a Perkin Elmer Spectrum One FTIR spectrophotometer (Bomem MB100). The lyophilized samples were evenly mixed with KBr in a 1:100 proportion and carefully pulverized in a clean, dry agate mortar. The powder was compressed using a tablet press and scanned in the energy range of 400 to 4000 cm^{-1} [15].

2.2.4 SEM analysis

The morphological structures of the prepared cryogel powder samples were examined employing a field emission scanning electron microscopy (FESEM)- energy dispersive X-ray spectroscopy (EDX) at an accelerating voltage of 15 KV (SEM; Philips XL30 ESEM) [16].

2.2.5 Antibacterial assessment employing disc diffusion assay

To evaluate the produced cryogels' antibacterial activity, an agar disc diffusion experiment was conducted. The cryogels made in the shape of discs were used for the study. The test strain overnight culture was employed to create bacterial suspensions (*E. coli*), which were then disseminated using sterile swabs on top of Luria Bertani (LB) agar plates after being adjusted to a turbidity of 0.5 McFarland standards [17]. Cryogels shaped into discs were placed onto LB agar plates seeded with *E. coli*. Wells were created for CFS, positive control (colistin, 5 mg/mL), and negative control (sterile water). Blank cryogels served as an additional control to evaluate the matrix's inherent activity. A positive control was examined. As a negative control, sterile distilled water was employed. A blank cryogel served as an additional control to evaluate the independent activity of the matrix. Positive control (5 mg/mL) and CFS (30 µL) were applied to each well. Upon completion of a 24-hour incubation at 37℃, the plates were inspected, and the widths of the inhibition zones surrounding the discs were measured to determine the antibacterial activity.

2.2.6 Determination of MIC using the broth dilution assay

The microdilution method, which was utilized in accordance with research [18] with minor adjustments, was used to compute the minimum inhibitory concentration (MIC). The lowest antibiotic concentration that prevents detectable planktonic bacterial cell development is known as the MIC. Each series of labelled test tubes received approximately 5 mL of LB broth before being injected with 10 µL of overnight culture (1×10^5 CFU/mL). About 20 µL of aseptic distilled water served as the negative control, and 20 µL of the respective positive control and control (CFS) were used in their labelled tubes. Cryogel powder was dispersed by vortexing in sterile broth for 5 min to ensure uniform suspension before addition. To the well-labelled treatment, 20 µl of cryogel powder was added at varying concentrations (5, 10, 20, 40, and 80 µg/mL) and maintained at 37℃ overnight. The lowest concentration at which no bacterial growth was detectable was taken as the MIC. Each test was run in triplicate.

2.2.7 Biofilm inhibition assay

Bacterial biofilm inhibition was conducted following [19], but with slight modifications. Each well in a 96-well microtiter plate was filled with 200 µL of LB broth, and each well was inoculated with 10 µL of bacterial culture, with the exception of the negative control. Positive control at different concentrations (¼ MIC, ½ MIC, and MIC) was studied. CFS (control) was analyzed in undiluted form. Cryogels were examined at varying concentrations (¼ MIC, ½ MIC, and MIC). Each well received 20 µL of the sample of their respective treatments. For 24 to 48 hr, the microtiter plates were maintained at 37℃. Following the incubation period, the medium was discarded, and phosphate-buffered saline (PBS) was added to the wells three times. The cells were stained with 0.1% crystal violet, which is meant to adhere to the wells, and then they were cleansed thrice employing PBS (pH 7.4). A plate reader (Genetix Ltd.) was then used to measure the absorbance of the eluate at 595 nm after the cell-bound dye had been eluted using around 200 µL of ethanol:acetone (80:20).

2.2.8 Congo red agar assay

The Congo red agar assay (CRA) was performed in accordance with the guidelines provided by study [20], but with a few adjustments. The culture isolate was grown on LB agar containing 5% (w/v) sucrose and 0.08% (w/v) Congo red. After autoclaving, the medium was combined with 100 µl of the treatment (CRYO) and the positive control. Each plate was filled with both treatments at MIC. Each plate was streaked with spots from the overnight culture, which was then maintained at 37℃ for 24 hr. The plates were inspected to check for the formation of any biofilm after incubation. Black colonies verify the creation of the biofilm. Red colonies are used to confirm which strains do not form biofilms. For cryo treatment, the culture was grown in a 5 mL LB broth containing powdered cryogel for 4 hr. The culture was then spotted on the plate.

2.2.9 ATP measurement assay

Following the manufacturer's instructions, the ATP luciferin-based assay (Sigma Aldrich, 119107) was used to quantify the amount of ATP in the bacterial cells as indicated

above, following treatment with cryogels (½ MIC and MIC). Cryogels at the specified MIC and inoculum (1×10^5 CFU/mL) were brought to a total volume of 100 µL and maintained for 4 hr at 37℃. The plates were incubated for 4 hr at 37℃. Following incubation, 50 µL of the sample was moved to a 96-well plate, and reconstitution buffer containing luciferase and substrate (luciferin) was added. Luminescence was quantified at 600 nm. The proportion of ATP production inhibition in CRYO-treated bacterial cells relative to control (untreated) cells was used to express the results.

2.2.10 Lipid peroxidation assay

Lipid peroxidation in the isolate was measured by employing the thiobarbituric acid reactive substance (TBARS) assay following [21]. Briefly, log-phase cultures of *E. coli* were exposed to ½ MIC and MIC of cryogels for 4 hr. The isolates were centrifuged and given a single wash with sterile distilled water after treatment. Glass beads were then added, and the pellets were vigorously vortexed after being resuspended in 200 µL of PBS (pH 6.8). After that, the contents were centrifuged at 25℃ for 8 minutes at 8000 rpm. The TBA reagent (0.5 M HCl, 12% trichloroacetic acid, and 0.375% thiobarbituric acid) was mixed with 1 mL of solution and maintained for 20 minutes at 90℃. A microtitre plate reader (Genetix, India) was utilized to quantify the absorbance at 535 nm after cooling. Malondialdehyde was used as a standard, and the outcomes were reported as µmoles of malondialdehyde (MDA)/mg of protein.

2.2.11 Real-time polymerase chain reaction (RT-PCR)

About 20 mL of the culture treated with cryo and positive control (MIC) in the previous section was used for the real-time expression. The HI Media RT PCR kit was used to extract and purify total RNA following the manufacturer's protocols. A UV spectrophotometer was used to determine the extracted total RNA concentrations (Shimadzu, 1800). The synthesis of cDNA was achieved utilizing random oligos. The HI Media cDNA reverse transcription kit was used to create cDNA from the isolated RNA, and Eppendorf systems were used for amplifying the result. The Corbett Research cycler (Bio-Rad) was utilized to quantify the samples (treated and control) in real time. Primers *ompA, ompF, ompC*, and *tolC* (Table 1) were employed in the amplification procedure at a concentration of 600 nM. Using 1.14 µl of the RNA products, the program ran for 40 cycles at 95℃ for 30 seconds (denaturation), 55℃ for 40 seconds (annealing), and with an elongation at 72℃ for 50 seconds. Together with the pertinent genes of interest, the housekeeping gene *recA* was amplified to compare the mRNA expression. The mRNA abundance within the experimental samples (including the control) was compared employing the Ct values (ΔΔCt method). The threshold cycle (Ct) values corresponding to the target gene were obtained and compared to its housekeeping gene.

2.2.12 Statistical analysis

Each experiment was run in triplicate. Two-way analysis of variance (ANOVA) was employed to evaluate the obtained data, and the Tukey test was employed to confirm that differences between samples were statistically significant ($p \leq 0.05$). Throughout the analysis, analyses were carried out using the Faculty Edition of the Statistical Package for the Social Sciences (SPSS) program.

Table 1. Nucleotide sequences of the primers employed for the study

Gene	Dir.	Sequence (5' – 3')	L	Tm (℃)	GC (%)	Product Size (kb)	Ref.
ompF	FW	CGTACTTCAGACCAGTAGCC	20	58.76	50	240	[19]
	RV	GAACTTCGCTGTTCAGTACC	20	58.73	50		
ompA	FW	TGGACCAACAACATCGGTGAC	20	58.99	50	210	[20]
	RV	CAACTACTGGAGCTGCTTCGC	20	59.05	55		
ompC	FW	CACAACAAGGCTGCCCATTC	20	60.04	55	470	This study
	RV	ATTGTTCTAGCAGTCGCCCC	20	60.11	55		
tolC	FW	AAGCCGAAAAACGCAACCT	20	58.98	55	217	[21]
	RV	CAGAGTCGGTAAGTGACCATC	20	58.91	55		
recA	FW	ATCTCCGTCAATCTCCGCAC	20	59	55	382	[22]
	RV	ACGCGCTGAACAAAAGGTTC	20	59.97	50		

Dir.: Direction; FW: Forward; RV: Reverse; L: Primer length; Tm: Melting temperature; GC: Guanine and cytosine content.

3. RESULTS AND DISCUSSION

3.1 Physical parameters of the synthesized cryogels

The synthesized cryogels were found to be porous and stable at room temperature for over 10 days (Figure 2).

3.2 FTIR analysis of chitosan-glutaraldehyde crosslinked polymers

The FTIR spectra shown in Figures 3(A, B) were utilized to investigate the structural configuration of chemical bonds of the polymers used and the structural alterations brought about by crosslinking with glutaraldehyde. The absorption bands for chitosan at about 2979.03 and 2888 cm^{-1} correspond to asymmetric and C-H symmetric stretching, respectively (Figure 3(A)). Amide I (C=O stretching), Amide II (N-H bending), and Amide III (C-N stretching) are responsible for the peaks detected at 1645.53, 1559, and 1381cm^{-1}, respectively [22]. The intensity and locations of the peaks were found to shift dramatically after the polymers were crosslinked in the presence of glutaraldehyde. The free amino group (amide A) and the OH group's absorption peak moved from 2979 to 3305 cm^{-1}. The chitosan and gelatine peaks overlapped to generate four strong absorption peaks in the spectra, which were located at 1645.57, 1551, 1410, and 1068 cm^{-1} (Figure 3(B)). Furthermore, during cross-linking, a novel absorption peak was produced at 1031 cm^{-1}, which was assigned to the C–O–C–O–C structure [23].

3.3 Antimicrobial activity of synthesized cryogels

With the cryogel (CRYO) formulation, strong antimicrobial activity was observed. Comparing CRYO to the positive

control, it demonstrated strong antibacterial action. Conversely, the control (CFS) had the least amount of antibacterial activity. There was a dose-dependent bactericidal activity ($p \leq 0.05$). For CFS, CRYO, and positive control ($p \leq 0.05$), the corresponding inhibition zones were 5.12 ± 0.18, 26.1 ± 1.04, and 34.45 ± 2.01. The enhanced inhibition observed with CRYO compared to CFS alone indicates a synergistic effect between chitosan's cationic nature and LAB-CFS metabolites.

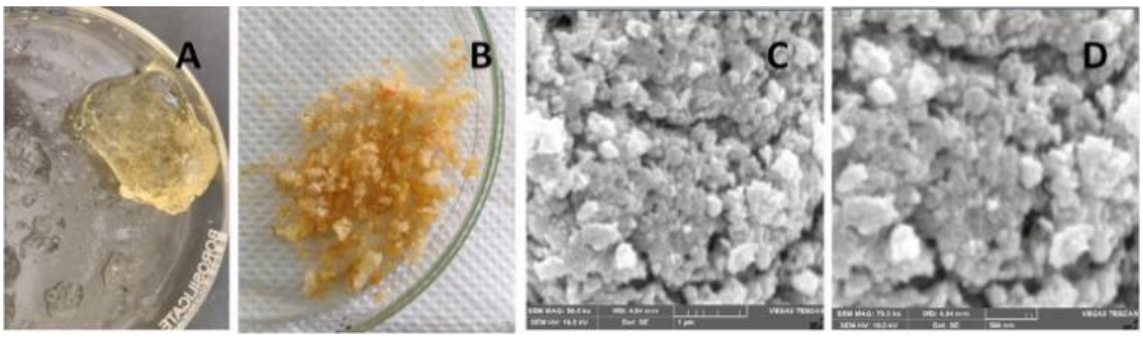

Figure 2. (A, B) The synthesized cryogels, and (C, D) The scanning electron microscopy images

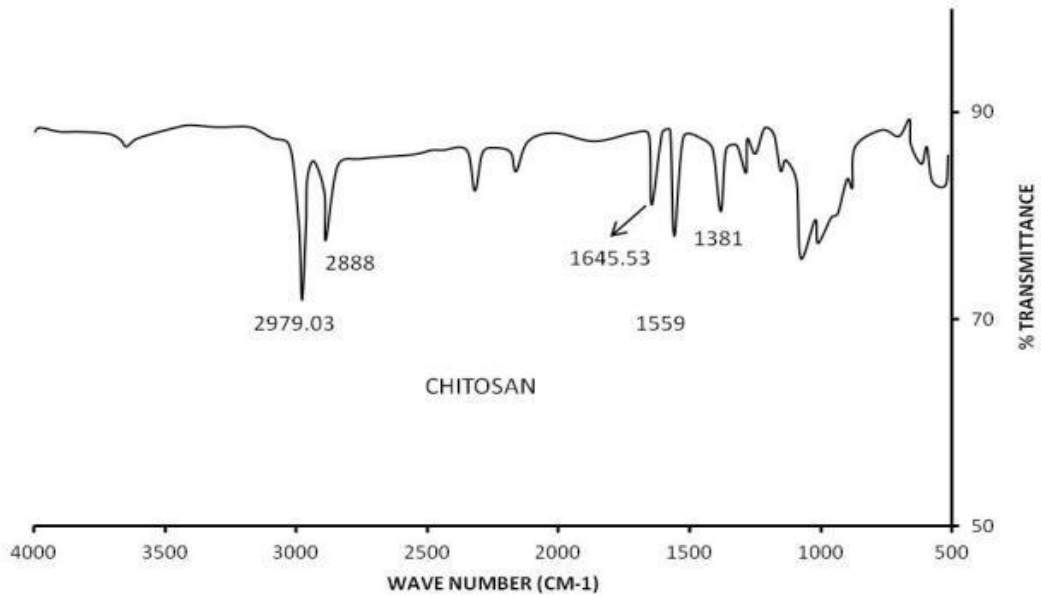

(A)

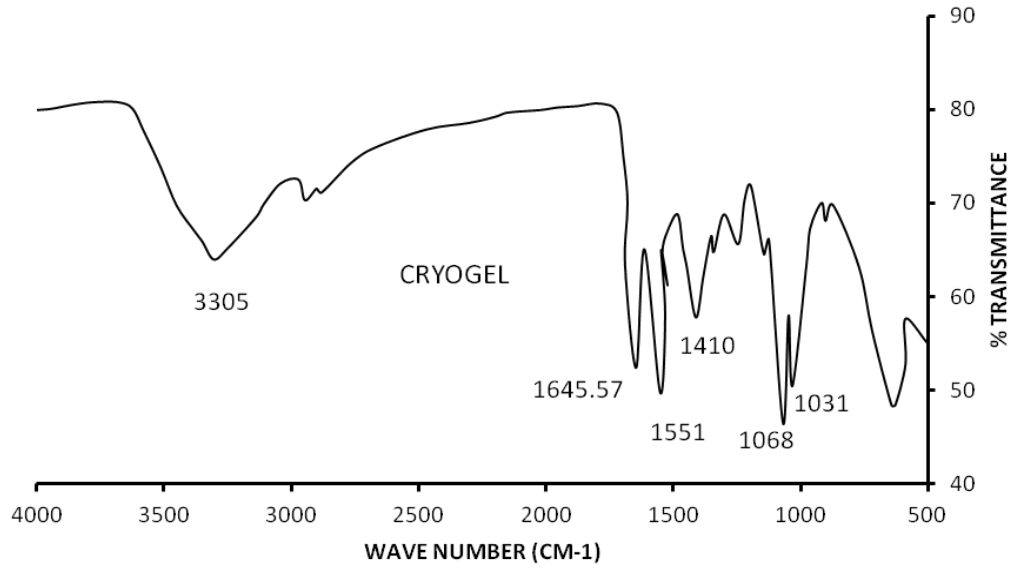

(B)

Figure 3. (A) FTIR spectra of chitosan, (B) FTIR spectra of cryogel synthesized with glutaraldehyde

3.4 Minimum inhibitory concentration of synthesized cryogels

From the results, the % inhibition of CRYO increased to 83% at 80 µg/mL when compared to the control (CFS; 42.7%) at 80 µg/mL. On the other hand, positive control showed 95% inhibition at the same concentration. The percent inhibition was found to be dose-dependent ($p \leq 0.05$) (Figure 4(A)). From this, MIC values were calculated to be 37.2 and 31.3 µg/mL, respectively, for CRYO and the positive control (Figure 4(B)). On the other hand, CFS showed 23% of MIC, which is significant but low when compared to the test and positive. This demonstrates that the CRYO formulation achieved a substantially lower MIC compared to CFS, confirming that integration into the cryogel matrix enhances antimicrobial potency.

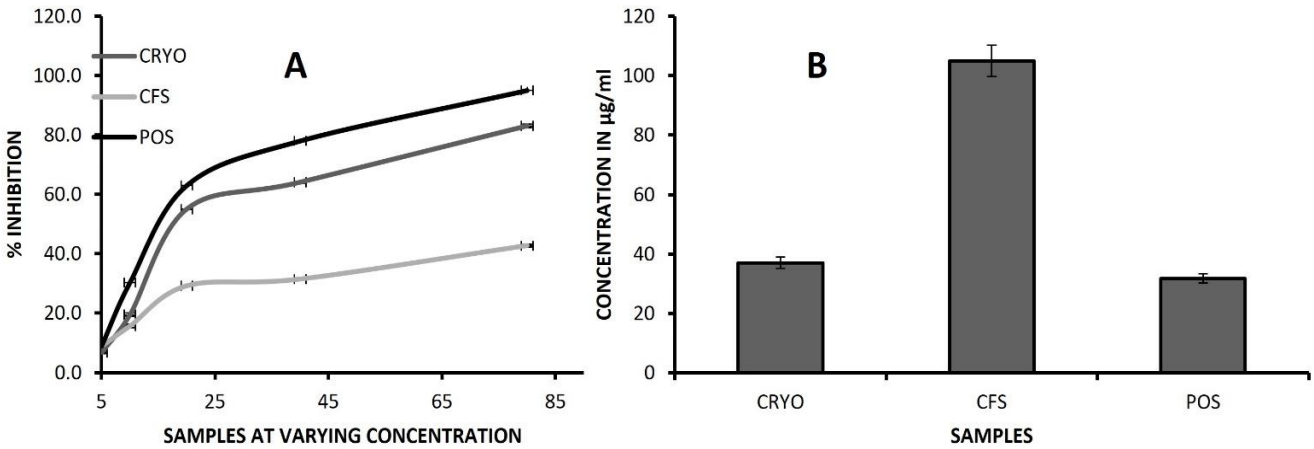

Figure 4. Comparing antimicrobial effectiveness among test samples: (A) Percent inhibition, (B) Minimum inhibitory values
CRYO: synthesized cryogels; CFS: cell-free supernatants; POS: positive control.

3.5 Antibiofilm activity of synthesized cryogels

The absorbance values for CRYO, POS, and CFSF at their respective MICs were determined to be 0.24 ± 0.035, 0.11 ± 0.021, and 0.81 ± 0.03512, respectively. For CRYO and POS, the percentage biofilm inhibition was 83 and 92%, respectively ($p \leq 0.05$), as presented in Figure 5. The CRA assay also confirmed the CRYO capacity to suppress biofilms. The dark colonies (Figure 6) indicate strong biofilm formation. Reddish coloured colonies on the CRYO and positive plates confirm the antibiofilm activity. This suggests that the CRYO formulation not only prevents bacterial growth but also disrupts biofilm establishment, an essential advantage over CFS or chitosan alone.

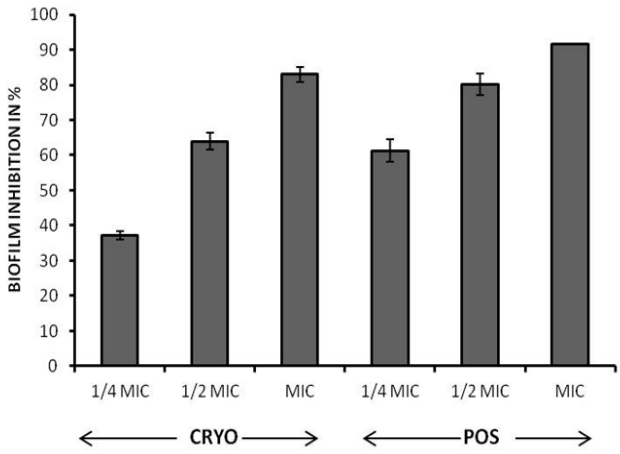

Figure 5. Percentage of biofilm inhibition
Colistin was utilized as a positive control. All the values are averages of triplicates.

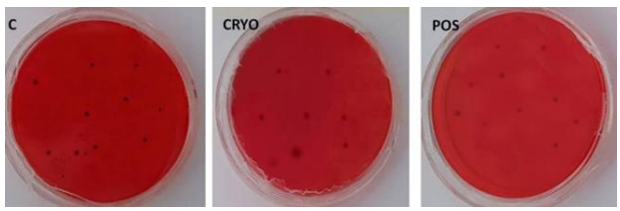

Figure 6. Colonies formed on the Congo red agar plates
C: control (black colonies); CRYO: synthesized cryogels; POS: positive control.

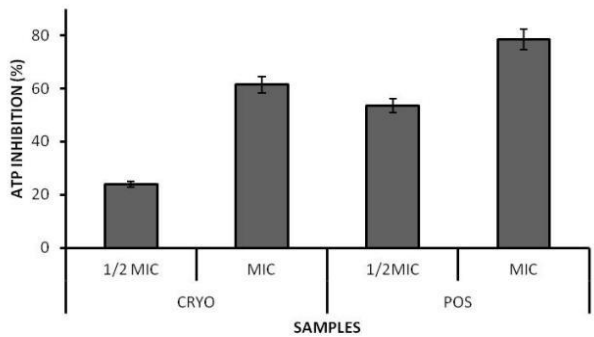

Figure 7. Toxicity of cryogels measured by ATP synthesis inhibition assay
Values are represented in percentage (%); Absorbance of the control was found to be 0.88.

3.6 Toxicity of cryogels as an antibacterial agent

The present research employed the measurement of ATP levels in bacterial cells to determine the toxicity of cryogels as a possible antibacterial agent. ATP levels were markedly reduced in the cryogel-treated *E. coli* (Figure 7) when compared to the positive control. Following treatment with the

MIC dosage of cryogels, bacterial cells' ATP production was significantly reduced. The percent inhibition was found to be 24 and 61%, respectively, for CRYO at ½ MIC and MICs ($p \leq 0.05$). On the other hand, positive control showed 78.5% inhibitions at MIC ($p \leq 0.05$). The significant decline in ATP levels implies metabolic suppression, likely due to oxidative stress and membrane damage induced by LAB metabolites and chitosan interaction.

3.7 Lipid peroxidation induced by cryogels

The results showed a significant rise in the lipid peroxidation as expressed in %. The lipid peroxidation for CRYO increased to 74% from 23% at MIC. The positive control showed 86% at MIC. The absorbance values were found to be 0.23 and 0.12, respectively, for CRYO and positive at MIC (Figure 8). The enhanced rise in the lipid peroxidation values signifies the amount of stress the isolates had during the treatment.

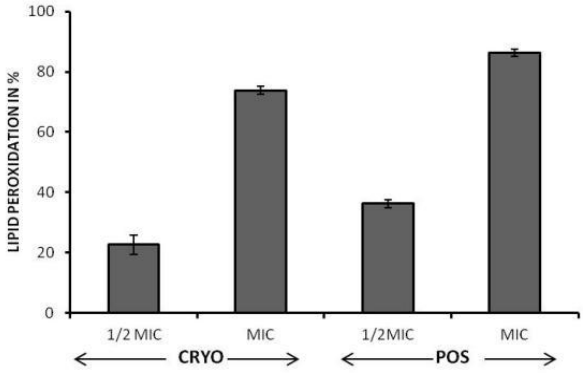

Figure 8. Lipid peroxidation values of the cryogels and the positive control

3.8 Expression of the outer membrane protein genes

The expression of the selected genes *ompA, ompF, ompC*, and *tolC,* as well as the housekeeping gene *recA,* was measured using RT-PCR. Figures 9 and 10 illustrate the down-regulation of the selected genes based on the transcriptional expression profile as measured by the Ct values. The observed patterns of expression aligned with the research on the suppression of biofilms *in vitro*. The results revealed that the virulence genes *ompA* and *ompF* were significantly down-regulated upon exposure to MIC of CRYO ($p \leq 0.05$). At the MIC level of CRYO, the relative expression levels of *ompA* and *ompF* were 0.87 and 0.78, respectively, compared to the control (1 or 100%). Conversely, *ompA* and *ompF* for the positive control were 0.76 and 0.81, respectively ($p \leq 0.05$). Similarly, it was found that, compared to the control (1 or 100%), the gene members associated with antimicrobial resistance (*ompC* and *tolC*) were significantly down-regulated. At the MIC level of CRYO, the relative expression amounts of *ompC* and *tolC* were 0.68 and 0.85, respectively, in comparison to the control (1 or 100%). The *ompC* and *tolC* values for the positive control were 0.68 and 0.82, respectively ($p \leq 0.05$). The findings were consistent with the studies on biofilm inhibition (Figure 11).

Over the past few decades, there has been a growing number of reports of antimicrobial resistance (AMR) in bacteria that cause UTIs, which has grown to be a serious public health concern. *Escherichia coli* [24], a widespread gram-negative bacterium and member of the Enterobacteriaceae family, is the most frequent cause of UTIs worldwide. One of the most prevalent extra-intestinal pathogenic *E. coli* (ExPEC) that are encountered is UPEC [25]. Mobile genetic elements (MGE), such as plasmids, insertion sequences, transposons, and gene cassettes/integrons, are commonly used by *E. coli* to acquire AMR genes [26].

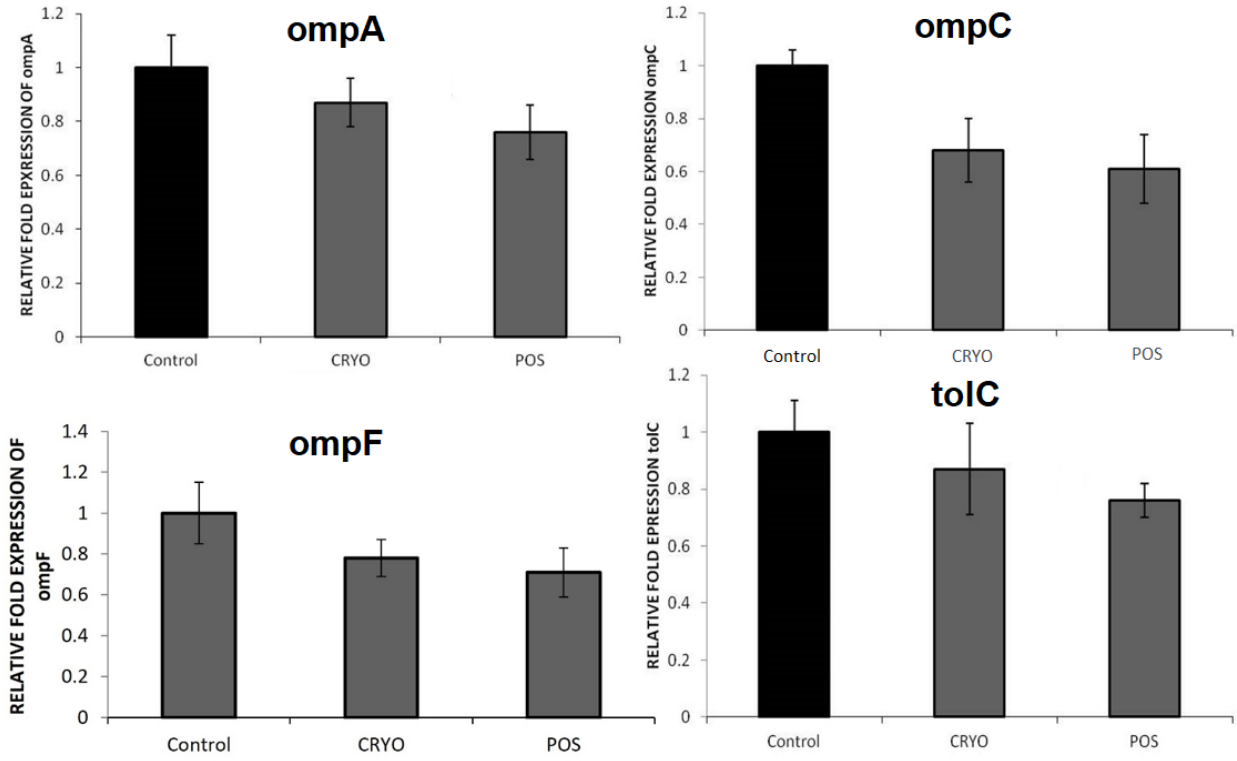

Figure 9. Histogram depicting RT-PCR's validation of the gene members
The *recA* gene was used as an internal reference (housekeeping gene) for normalization of gene expression. All experiments were conducted in triplicate.

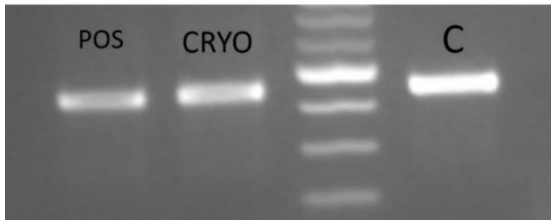

Figure 10. Agarose gel (1%) image showing the expressed DNA bands of the *ompC* gene member on treatment with cryogels (CRYO), positive control (POS), and control (C)

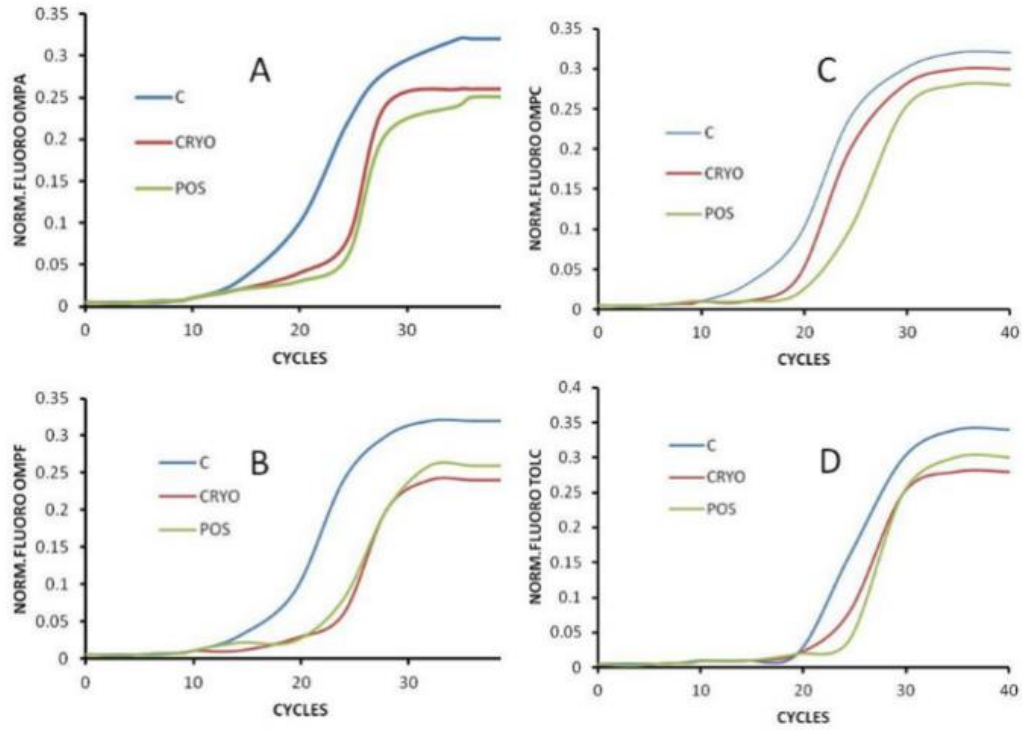

Figure 11. CT curves depicting RT-PCR's validation of the gene members

The *recA* gene was used as an internal reference (housekeeping gene) for normalization of gene expression. All experiments were conducted in triplicate. A: *ompA*; B: *ompF*; C: *ompC*; D: *tolC*

Antibiotic-loaded cryogels are macroporous polymer networks created by freeze-thaw cycles that act as drug carriers for the local, regulated administration of antibiotics, frequently in tissue engineering or wound healing applications. Antibiotics incorporated into cryogels are absorbed and released under controlled conditions due to their porous structure. Over time, the antibiotic diffuses out of the gel matrix to do this. Antibiotics can be locally administered at the infection site by loading them directly into a cryogel [27]. This increases drug concentration at the target and lessens the requirement for systemic (oral, for example) antibiotic treatment. Additionally, the antibiotic's presence in the cryogel may improve efficacy and may overcome bacterial resistance by delivering a long-lasting therapeutic effect at the infection site [28].

Significant antibacterial activity was observed for the CRYO formulation. The CRYO showed strong antibacterial activity as compared to the positive control. In contrast to the positive control, it was discovered that the manufactured cryogels did release the antimicrobial chemicals and were visible with the clear zone ($p \leq 0.05$). The synthesised cryogels demonstrated a minimal MIC of 37.2 µg/mL (Figure 4(B)), which is highly significant in relation to the positive control ($p \leq 0.05$), and bacterial growth inhibition was confirmed through broth dilution. In accordance with MICs, biofilm inhibition was investigated. Comparing the synthesized CRYO to the positive control (92%) showed a significant (83%) inhibition of biofilm development ($p \leq 0.05$). The CRA assay, which showed brownish to light brown colonies after treatment with the cryogels, also validated the assay.

Assays for lipid peroxidation and ATP measurement were used to assess the antibacterial properties of the bacterial cells after they were treated with cryogels. When compared to the positive control, the cryogel-treated *E. coli* showed a significant decrease in ATP levels. At the cryogels' MIC, a 61% decrease in ATP levels ($p \leq 0.05$) was observed. The level of stress that the isolates experienced during treatment was indicated by the notable increase (Figure 7) in lipid peroxidation (74%) at MIC that was observed.

Based on the qPCR analyses, it was discovered that the study's gene components were significantly down-regulated upon exposure to CRYO ($p \leq 0.05$). Comparing *ompA* and *ompF* to the control (1 or 100%), they were decreased to 0.87 and 0.78, respectively (Figure 9). Compared to the control (1 or 100%), the relative expression levels of *ompC* and *tolC* at MIC were 0.68 and 0.85, respectively. The results align with the biofilm inhibition research.

Studies verify that different kinds of cryogels successfully

stop bacteria from growing, especially when antimicrobial chemicals are added. These cutting-edge biomaterials are utilized in biomedical scaffolds, active food packaging, and wound dressings [6, 29]. The main mechanism of bactericidal chemicals' antibacterial action is their regulated release. Research has demonstrated that within two hr, pullulan cryogels containing the antibiotic ciprofloxacin can totally stop the growth of *Staphylococcus aureus* and *Escherichia coli* [30]. Carboxymethyl chitosan (CMC) cryogels laden with ciprofloxacin are designed to deliver the antibiotic in a regulated way in proportions that are adequate to totally stop *Klebsiella oxytoca* from growing [31]. It is claimed that calcium peroxide (CP) microparticle cryogels limit the growth of bacteria resistant to antibiotics, such as MRSA and *Pseudomonas aeruginosa*, and emit hydrogen peroxide [32]. *Staphylococcus aureus and E. coli* have been shown to be significantly inhibited by silver nanoparticle-containing cryogels, such as hybrid polyacrylamide-AgNPs and recombinant keratin-chitosan cryogels coated with gallic acid-reduced AgNPs [33]. Tests have demonstrated that ceftriaxone-loaded poly(vinyl alcohol) cryogels can effectively cure infected wounds by forming a "growth inhibition zone" against *Staphylococcus aureus* and *E. coli,* serving as transient antimicrobial implants [34].

According to reports, a variety of nanoparticles can cause bacteria to express fewer outer membrane proteins (OMPs), which can increase membrane permeability and prevent the growth of germs. This action is a key component of some nanoparticles' antibacterial function. Research conducted on *Escherichia coli* demonstrates that exposure to AgNPs can cause resistant bacterial strains to express fewer OMPs, such as *OmpC* and *OmpF* [35]. Although their effectiveness may vary depending on the species, chitosan nanoparticles (CSNPs) are efficient against both Gram-positive and Gram-negative bacteria. According to reports on *E. coli*, CSNPs may have antibacterial properties by preventing the formation of outer membranes and metabolic processes. Genes linked to DNA absorption and processing, including those involved in cell membrane permeability (*ompA* and *ompC*), have been shown to have their expression downregulated in *E. coli* when exposed to low concentrations of CeO_2 nanoparticles. This is connected to a decrease in membrane permeability and reactive oxygen species (ROS) [36]. It has been observed that titanium dioxide (TiO_2) nanoparticles alter the expression of outer membrane proteins in *E. coli* [37].

One of the main mechanisms of chitosan nanoparticles' (CNPs) antibacterial action is the downregulation of outer membrane proteins (OMPs) in bacteria. Protein synthesis and function are impacted when the positively charged CNPs attach to the negatively charged bacterial surface, changing the permeability of the cell membrane. According to a recent study, silver nanoparticles coated with chitosan can attach to UPEC adhesins, such as *PapG* and *FimH*. According to this interaction, chitosan may prevent bacterial attachment and colonization by interfering with particular outer membrane proteins involved in adhesion [38]. Chitosan nanoparticles dramatically reduced the expression of the genes (*LasI* and *RhlI*) that control virulence factors in *P. aeruginosa*. As a result, these vital genes were downregulated, motility was decreased, and biofilms were formed [39]. The effect of deacetylated chitosan on *P. aeruginosa* and *S. aureus* was investigated in a 2011 study. The leaking of intracellular contents, including soluble proteins, demonstrated that chitosan enhanced cell membrane permeability [40].

On the basis of available information, there have been reports of nanoparticles working against UPEC by inhibiting the expression of outer membrane proteins. Numerous reports of chitosan-based nanoparticles have confirmed their promise as antibacterial agents, particularly against strains of UPEC. However, very little information about the application of cryogels against UPEC strains, particularly to target the expression patterns of the outer membrane proteins, has been published.

The absence of a blank control in our confirmatory studies is one of the study's limitations. This choice was made in light of the unfavourable outcomes of our preliminary experiments (MIC), which indicated that the blank control would not produce useful data. However, we are unable to completely rule out background effects or minute experimental artifacts due to the lack of a blank control. Future research using suitable blank controls might improve the findings' dependability and offer a more thorough validation of the observed results.

4. CONCLUSION

The findings of the present study showed that the synthesized cryogels were stable, porous, and demonstrated clear antibacterial, antibiofilm, and antivirulence effects against clinical isolates of UPEC. The drug-loaded cryogels are intended for further evaluation as short-term implants with potential effects on tissue recovery following the removal of the corresponding gel insertions. Cell-free supernatant was utilized as the antibacterial agent to develop chitosan-coated cryogels through a simple freeze–thaw process. The cryogels prepared showed high antibacterial activity, high biofilm formation inhibition, and virulence gene associated with the outer membrane protein (*ompA*, *ompF*, *ompC*, and *tolC*) repression. All these findings indicate the multifunctional efficacy of the formed cryogels in breaking bacterial virulence and resistance mechanisms. These cryogels, based on their performance and biocompatibility, can be used as a topical antimicrobial coating on urinary catheters, wound dressings, or localized sources of prevention of infection in implants. It should also be stressed that these findings need further validation in terms of the protein expression research, and further investigation to determine the effect of these materials is necessary using both *in vivo* and *ex vivo* studies.

REFERENCES

[1] Luna-Pineda, V.M., Ochoa, S.A., Cruz-Cordova, A., Cazares-Dominguez, V., Reyes-Grajeda, J.P., Flores-Oropeza, M.A., Xicohtencatl-Cortes, J. (2018). Features of urinary Escherichia coli isolated from children with complicated and uncomplicated urinary tract infections in Mexico. PloS One, 13(11): e0208285. https://doi.org/10.1371/journal.pone.0208285

[2] Whelan, S., Lucey, B., Finn, K. (2023). Uropathogenic Escherichia coli (UPEC)-associated urinary tract infections: the molecular basis for challenges to effective treatment. Microorganisms, 11(9): 2169. https://doi.org/10.3390/microorganisms11092169

[3] Lupo, F., Ingersoll, M.A., Pineda, M.A. (2021). The glycobiology of uropathogenic E. coli infection: The sweet and bitter role of sugars in urinary tract immunity.

Immunology, 164(1): 3-14. https://doi.org/10.1111/imm.13330
[4] Memic, A., Colombani, T., Eggermont, L.J., Rezaeeyazdi, M., Steingold, J., Rogers, Z.J., Bencherif, S.A. (2019). Latest advances in cryogel technology for biomedical applications. Advanced Therapeutics, 2(4): 1800114. https://doi.org/10.1002/adtp.201800114
[5] Xiang, J., Shen, L., Hong, Y. (2020). Status and future scope of hydrogels in wound healing: Synthesis, materials and evaluation. European Polymer Journal, 130: 109609. https://doi.org/10.1016/j.eurpolymj.2020.109609
[6] Kolosova, O.Y., Shaikhaliev, A.I., Krasnov, M.S., Bondar, I.M., Sidorskii, E.V., Sorokina, E.V., Lozinsky, V.I. (2023). Cryostructuring of polymeric systems: 64. Preparation and properties of poly (vinyl alcohol)-based cryogels loaded with antimicrobial drugs and assessment of the potential of such gel materials to perform as gel implants for the treatment of infected wounds. Gels, 9(2): 113. https://doi.org/10.3390/gels9020113
[7] Prete, S., Dattilo, M., Patitucci, F., Pezzi, G., Parisi, O.I., Puoci, F. (2023). Natural and synthetic polymeric biomaterials for application in wound management. Journal of Functional Biomaterials, 14(9): 455. https://doi.org/10.3390/jfb14040455
[8] Feng, P., Luo, Y., Ke, C., Qiu, H., Wang, W., Zhu, Y., Wu, S. (2021). Chitosan-based functional materials for skin wound repair: Mechanisms and applications. Frontiers in Bioengineering and Biotechnology, 9: 650598. https://doi.org/10.3389/fbioe.2021.650598
[9] Ojeda-Hernández, D.D., Canales-Aguirre, A.A., Matias-Guiu, J., Gomez-Pinedo, U., Mateos-Díaz, J.C. (2020). Potential of chitosan and its derivatives for biomedical applications in the central nervous system. Frontiers in Bioengineering and Biotechnology, 8: 389. https://doi.org/10.3389/fbioe.2020.00389
[10] Arena, M.P., Silvain, A., Normanno, G., Grieco, F., Drider, D., Spano, G., Fiocco, D. (2016). Use of Lactobacillus plantarum strains as a bio-control strategy against food-borne pathogenic microorganisms. Frontiers in Microbiology, 7: 464. https://doi.org/10.3389/fmicb.2016.00464
[11] Liu, G., Kragh, M.L., Aabo, S., Jensen, A.N., Olsen, J.E. (2022). Inhibition of virulence gene expression in Salmonella Dublin, Escherichia coli F5 and Clostridium perfringens associated with neonatal calf diarrhea by factors produced by lactic acid bacteria during fermentation of cow milk. Frontiers in Microbiology, 13: 828013. https://doi.org/10.3389/fmicb.2022.828013
[12] Efthimiou, G., Tsiamis, G., Typas, M.A., Pappas, K.M. (2019). Transcriptomic adjustments of Staphylococcus aureus COL (MRSA) forming biofilms under acidic and alkaline conditions. Frontiers in Microbiology, 10: 2393. https://doi.org/10.3389/fmicb.2019.02393
[13] Masebe, R.D., Thantsha, M.S. (2022). Anti-biofilm activity of cell free supernatants of selected lactic acid bacteria against Listeria monocytogenes isolated from avocado and cucumber fruits, and from an avocado processing plant. Foods, 11(18): 2872. https://doi.org/10.3390/foods11182872
[14] Ayaz, F., Demir, D., Bölgen, N. (2021). Differential anti-inflammatory properties of chitosan-based cryogel scaffolds depending on chitosan/gelatin ratio. Artificial Cells, Nanomedicine, and Biotechnology, 49(1): 682-690. https://doi.org/10.1080/21691401.2021.2012184
[15] Li, D., Cui, H., Hayat, K., Zhang, X., Ho, C.T. (2022). Superior environmental stability of gelatin/CMC complex coacervated microcapsules via chitosan electrostatic modification. Food Hydrocolloids, 124: 107341. https://doi.org/10.1016/j.foodhyd.2021.107341
[16] Shu, X., Liu, J., Mao, L., Yuan, F., Gao, Y. (2024). Composite hydrogels filled with rhamnolipid-based nanoemulsion, nanostructured lipid carrier, or solid lipid nanoparticle: A comparative study on gel properties and the delivery of lutein. Food Hydrocolloids, 146: 109264. https://doi.org/10.1016/j.foodhyd.2023.109264
[17] Driscoll, A.J., Bhat, N., Karron, R.A., O'Brien, K.L., Murdoch, D.R. (2012). Disk diffusion bioassays for the detection of antibiotic activity in body fluids: applications for the pneumonia etiology research for child health project. Clinical Infectious Diseases, 54(suppl_2): S159-S164. https://doi.org/10.1093/cid/cir1061
[18] Mouzaki, M., Maroui, I., Mir, Y., Lemkhente, Z., Attaoui, H., El Ouardy, K., Mouine, H. (2022). Green synthesis of silver nanoparticles and their antibacterial activities. Green Processing and Synthesis, 11(1): 1136-1147. https://doi.org/10.1515/gps-2022-0061
[19] Irayyif, S.M., Senthil Kumar, R., Malla, S. (2014). Identification of methicillin resistant Staphylococcus aureus by a rapid polymerase chain reaction technique. Asian Journal of Pharmaceutical and Clinical Research, 7(5): 16-19.
[20] Cotter, J.J., O'Gara, J.P., Mack, D., Casey, E. (2009). Oxygen-mediated regulation of biofilm development is controlled by the alternative sigma factor σB in Staphylococcus epidermidis. Applied and Environmental Microbiology, 75(1): 261-264. https://doi.org/10.1128/AEM.00261-08
[21] Viveiros, M., Dupont, M., Rodrigues, L., Couto, I., Davin-Regli, A., Martins, M., Amaral, L. (2007). Antibiotic stress, genetic response and altered permeability of E. coli. PloS One, 2(4): e365. https://doi.org/10.1371/journal.pone.0000365
[22] van der Westhuizen, W.A., Theron, C.W., Boucher, C.E., Bragg, R.R. (2019). Regulation of outer-membrane proteins (OMPs) A and F, during hlyF-induced outer-membrane vesicle (OMV) biosynthesis. Heliyon, 5(7): e02014. https://doi.org/10.1016/j.heliyon.2019.e02014
[23] Swick, M.C., Morgan-Linnell, S.K., Carlson, K.M., Zechiedrich, L. (2011). Expression of multidrug efflux pump genes acrAB-tolC, mdfA, and norE in Escherichia coli clinical isolates as a function of fluoroquinolone and multidrug resistance. Antimicrobial Agents and Chemotherapy, 55(2): 921-924. https://doi.org/10.1128/AAC.00996-10
[24] Sharma, S., Malla, S. (2020). Molecular docking and ADME analysis for anti-HIV1 potential of Quassimolds from *Simarouba glauca*. Journal of Pharmaceutical and Clinical Research, 8(4): 555742. https://juniperpublishers.com/jpcr/pdf/JPCR.MS.ID.555742.pdf.
[25] Bölgen, N., Demir, D., Öfkeli, F., Ceylan, S. (2016). Extraction and characterization of chitin and chitosan from blue crab and synthesis of chitosan cryogel scaffolds. Journal of the Turkish Chemical Society Section A: Chemistry, 3(3): 131-144. https://doi.org/10.18596/jotcsa.00634

[26] Qian, Y.F., Zhang, K.H., Chen, F., Ke, Q.F., Mo, X.M. (2011). Cross-linking of gelatin and chitosan complex nanofibers for tissue-engineering scaffolds. Journal of Biomaterials Science, Polymer Edition, 22(8): 1099-1113. https://doi.org/10.1163/092050610X499447

[27] Raeispour, M., Ranjbar, R. (2018). Antibiotic resistance, virulence factors and genotyping of Uropathogenic Escherichia coli strains. Antimicrobial Resistance & Infection Control, 7(1): 118. https://doi.org/10.1186/s13756-018-0411-4

[28] Bien, J., Sokolova, O., Bozko, P. (2012). Role of uropathogenic Escherichia coli virulence factors in development of urinary tract infection and kidney damage. International Journal of Nephrology, 2012(1): 681473. https://doi.org/10.1155/2012/681473

[29] Calhau, V., Domingues, S., Ribeiro, G., Mendonça, N., Da Silva, G.J. (2015). Interplay between pathogenicity island carriage, resistance profile and plasmid acquisition in uropathogenic Escherichia coli. Journal of Medical Microbiology, 64(8): 828-835. https://doi.org/10.1099/jmm.0.000104

[30] Ari, B., Sahiner, M., Suner, S.S., Demirci, S., Sahiner, N. (2023). Super-macroporous pulluan cryogels as controlled active delivery systems with controlled degradability. Micromachines, 14(7): 1323. https://doi.org/10.3390/mi14071323

[31] Mykolayovych, S.A. (2021). Mathematical substantiation of the technology of creating a pharmaceutical composition in the form of cryogel. Pharmacophore, 12(5): 98-105. https://doi.org/10.51847/tlEfQhySJf

[32] Chaux-Gutiérrez, A.M., Pérez-Monterroza, E.J., Cattelan, M.G., Janzantti, N.S., Nicoletti, V.R., Aouada, F.A., de Moura, M.R. (2025). Active packaging incorporating cryogels loaded with pink pepper essential oil (Schinus terebinthifolius Raddi) for strawberry preservation. Processes, 13(4): 1179. https://doi.org/10.3390/pr13041179

[33] Chen, L., Xie, Y., Chen, X., Li, H., Lu, Y., Yu, H., Zheng, D. (2024). O-carboxymethyl chitosan in biomedicine: A review. International Journal of Biological Macromolecules, 275: 133465 https://doi.org/10.1016/j.ijbiomac.2024.133465

[34] Dar, L.A., Manzoor, T., Shafi, S., Kumar, A., Ahmad, S.M. (2024). Fabrication and characterization of calcium peroxide and berberine loaded cryogels for enhanced wound healing. Journal of Materials Chemistry B, 12(34): 8431-8443. https://doi.org/10.1039/d4tb00989d

[35] Carvalho, B.M.A., Da Silva, S.L., Da Silva, L.H.M., Minim, V.P.R., Da Silva, M.C.H., Carvalho, L.M., Minim, L.A. (2014). Cryogel poly (acrylamide): Synthesis, structure and applications. Separation & Purification Reviews, 43(3): 241-262. https://doi.org/10.1080/15422119.2013.795902

[36] Privar, Y., Shashura, D., Pestov, A., Modin, E., Baklykov, A., Marinin, D., Bratskaya, S. (2019). Metal-chelate sorbents based on carboxyalkylchitosans: Ciprofloxacin uptake by Cu (II) and Al (III)-chelated cryogels of N-(2-carboxyethyl) chitosan. International Journal of Biological Macromolecules, 131: 806-811. https://doi.org/10.1016/j.ijbiomac.2019.03.122

[37] Bruna, T., Maldonado-Bravo, F., Jara, P., Caro, N. (2021). Silver nanoparticles and their antibacterial applications. International Journal of Molecular Sciences, 22(13): 7202. https://doi.org/10.3390/ijms22137202

[38] Anthony, E.T., Ojemaye, M.O., Okoh, A.I., Okoh, O.O. (2020). Synthesis of CeO_2 as promising adsorbent for the management of free-DNA harboring antibiotic resistance genes from tap-water. Chemical Engineering Journal, 401: 125562. https://doi.org/10.1016/j.cej.2020.125562

[39] Lin, X., Li, J., Ma, S., Liu, G., Yang, K., Tong, M., Lin, D. (2014). Toxicity of TiO_2 nanoparticles to Escherichia coli: effects of particle size, crystal phase and water chemistry. PloS One, 9(10): e110247. https://doi.org/10.1371/journal.pone.0110247

[40] Mendez-Pfeiffer, P., Ballesteros-Monrreal, M.G., Juarez, J., Gastelum-Cabrera, M., Martinez-Flores, P., Taboada, P., Valencia, D. (2024). Chitosan-coated silver nanoparticles inhibit adherence and biofilm formation of Uropathogenic Escherichia coli. ACS Infectious Diseases, 10(4): 1126-1136. https://doi.org/10.1021/acsinfecdis.3c00229